Evaluations of prestack anisotropic Kirchhoff, phase-shift-plus-interpolation and reverse-time depth migration methods for dipping TI media

Xiang Du, John C. Bancroft, Don C. Lawton and Larry R .Lines, CREWES, University of Calgary*

Summary

Thick anisotropic sequences of dipping sandstones and shales often overlie reservoirs in fold and thrust belts, such as the Canadian Foothills. In these cases, such an assumption, when anisotropy is negligible or only anisotropy with vertical symmetry axis (VTI) is considered, may result in imaging problems and mispositioning errors. Three prestack anisotropic migration algorithms based on totally different principles, Kirchhoff, phase-shift-plus-interpolation (PSPI) and reverse-time (RT), are presented for dipping TI media. Derived from the isotropic Kirchhoff, PSPI and reverse-time migration methods, these three algorithms each inherit different characteristics of accuracy and efficiency. The ray-tracing algorithm used in 2-D prestack Kirchhoff depth migration is modified to calculate the traveltime in the presence of TI media with a tilted symmetry axis. Based on an analytical solution of vertical wavenumber for dipping TI media and an assumption for the relationship between anisotropic parameters versus lateral velocities, the prestack anisotropic PSPI migration can handle lateral variable anisotropic parameters and velocities. The prestack anisotropic reverse-time algorithm employs the weak-anisotropy approximation to obtain the individual P wave equation and implements depth migration with the pseudo-spectral method. An example of migration on physical data with these three algorithms shows improved imaging results from considering anisotropy parameters and different characteristics for each method.

Introduction

Hydrocarbon resource exploration and development projects are in areas containing dipping anisotropic sequences, such as in the Canadian Foothills (Isaac and Lawton, 1999). In these cases, depth migrations with either an isotropic migration algorithm or a vertical axis of symmetry (VTI) assumption will result in imaging problems and mispositioning errors. Anisotropic depth migration is required to correctly locate images when dipping transversely isotropic (TI) strata are present. Some advanced migration methods have been extended from isotropic to anisotropic media. Anisotropic depth migration methods, as with isotropic methods, can be based on various approaches such as ray-tracing, one-way equation, and full-wave equation. The prestack anisotropic Kirchhoff migration method presented in this paper is based on the ray-tracing theory. The prestack anisotropic PSPI starts from the one-way wave equation and carried out downward-continued wavefield extrapolation. Prestack anisotropic reverse-time migration achieves recursive extrapolation backward in time with the full wave equation. Three representative methods are chosen to demonstrate the characteristics of Kirchhoff, PSPI and reverse-time migration for dipping TI media in terms of performance, accuracy and efficiency. In this paper, we will first introduce the theory of three anisotropic migration methods, give certain analysis for each algorithm, and take into account the increase in calculation time between each anisotropic migration algorithm and the corresponding isotropic case. Through a physical model example, we demonstrate the performance of anisotropic migration algorithms and give some evaluations of these three anisotropic migration methods.

Theory

To illustrate the difference among anisotropic Kirchhoff, PSPI and reverse-time migration algorithms, we focus on the core techniques for each anisotropic algorithm.

Anisotropic Kirchhoff depth migration

The difference between the anisotropic and isotropic Kirchhoff migration algorithms lies in the traveltime calculation without changing the Kirchhoff algorithm itself. In this paper, a ray-tracing method (Kirtland Grech, 2002) is adopted to obtain traveltime tables for Kirchhoff depth migration. We start from the P-wave phase velocity equation (Tsvankin, 1996) written as

$$\frac{v^2(\theta)}{v_{p0}^2} = 1 + \varepsilon \sin^2\theta - \frac{f}{2} + \frac{f}{2}\sqrt{\left(1 + \frac{2\varepsilon \sin^2\theta}{f}\right) - \frac{2(\varepsilon - \delta)\sin^2 2\theta}{f}}, \quad (1)$$

where v is phase velocity, as a function of phase angle θ, v_{p0} is vertical quasi-P wave velocity, v_{s0} is quasi-S wave velocity, $f = 1 - v_{s0}^2 / v_{p0}^2$ and ε and δ are Thomsen's parameters (Thomsen, 1986). Since we consider the depth migration algorithms for P-waves, with the linear weak anisotropy approximation, the phase velocity of P-waves is

$$v_p(\theta) = a_0(1 + \delta \sin^2\theta \cos^2\theta + \varepsilon \sin^4\theta). \quad (2)$$

The corresponding derivative $dv_p(\theta)/d\theta$ is computed as

$$\frac{dv_p(\theta)}{d\theta} = a_0\left\{2\delta[\cos^3\theta \sin\theta - \cos\theta \sin^3\theta] + 4\varepsilon \cos\theta \sin^3\theta\right\}. \quad (3)$$

The relationship between the phase and group velocity is shown in equation (3) and (4)

$$g = \sqrt{v_p^2 + \left(\frac{\partial v_p}{\partial \theta}\right)^2} \tag{4}$$

and

$$\phi = \theta + \tan^{-1}\left(\frac{\partial v_p / \partial \theta}{v}\right) \tag{5}$$

where g is group velocity of P-wave, ϕ is the angle between the group velocity and symmetry axis and θ is the angle between the phase velocity and symmetry axis. For anisotropic ray-tracing, we undertake tracing a ray across an interface with different anisotropy parameters according to Snell's law. Figure 1 illustrates the relationship among phase angle θ, ray angle ϕ, incident phase angle β, and incident ray angle α. At the same time, it can be found that

$$\alpha = \phi + \gamma, \qquad \beta = \theta + \gamma, \tag{6}$$

where γ is the angle of the TI symmetry axis. From each source position, a set of rays are traced. When rays intersect an interface, the phase angles are determined through a scanning calculation and interpolation with Equation (5) for a range of phase angle from 0^0 to 90^0. Since the ray parameter p is constant for a given ray across an interface, which is calculated from

$$p = \frac{\sin(\theta + \gamma)}{v(\theta)}, \tag{7}$$

we use the same method to obtain the refracted phase angle. In each layer, the Equation (4) is used to obtain the group velocity. Consequently the traveltime is generated from the ray path length over the group velocity.

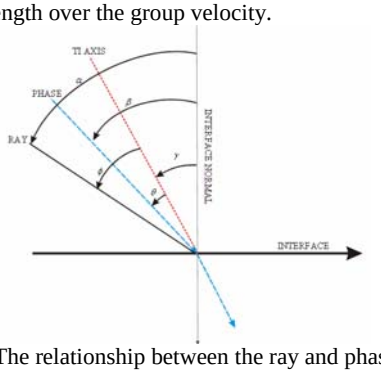

Figure 1. The relationship between the ray and phase angles with the TI axis.

Anisotropic PSPI depth migration

Extending the isotropic PSPI algorithm to anisotropic PSPI algorithm depends on two key techniques. One is the vertical wavenumber calculation. The other is the assumption of the number of reference anisotropy parameters. As for the first topic, we start from the frequency-dispersion equation. Similar to the isotropic case, we have the dispersion relationship in dipping TI media:

$$k_z = \pm\sqrt{\frac{\omega^2}{v^2(\theta,\phi)} - k_x^2}, \tag{8}$$

where ω is the frequency, $v(\theta,\phi)$ is the angle-dependent velocity, θ is the phase angle with the symmetry axis, and ϕ is the dipping angle of TI media. In the isotropic case, ω and v are constant, so k_z can be readily computed. In anisotropic media, the angle-dependence of velocity makes the computation more complicated. Le Rousseau (1991) precomputed a table of $k_z(\theta)$ and $k_x(\theta)$, and then locates or interpolates a given input k_x in the table, to find the corresponding k_z .The accuracy of this table-driven algorithm is directly related to the size of the table. Ferguson and Margrave (1998) suggested using an interpolating polynomial to get approximate solutions of k_z. It seems that experiments are cumbersome with difference anisotropic parameters. In fact, we can solve k_z analytically from the quartic dispersion equation. With Equation (1), when we rotate the symmetry axis from vertical to a titled angle ϕ, the phase velocity of the P-wave in the direction measured from the vertical direction is:

$$\frac{v^2(\theta,\phi)}{v_{p0}^2} = 1 + \varepsilon\sin^2(\theta-\phi) - \frac{f}{2} + \frac{f}{2}\sqrt{\left(1 + \frac{2\varepsilon\sin^2(\theta-\phi)}{f}\right)^2 - \frac{2(\varepsilon-\delta)\sin^2 2(\theta-\phi)}{f}}. \tag{9}$$

From Equation (8), for plane waves traveling in the vertical (x, z)-plane, the phase angle is given by

$$\sin\theta = \frac{v(\theta,\phi)k_x}{\omega}, \quad \cos\theta = \frac{v(\theta,\phi)k_z}{\omega} \tag{10}$$

Substituting Equation (10) into Equation (9), we can obtain the quartic equation

$$k_z^4 + a_3 k_z^3 + a_2 k_z^2 + a_1 k_z^1 + a_0 = 0, \tag{11}$$

where a_i ($i = 0, 1, 2, 3$) is related to k_x, ε, δ, v_{p0} and ϕ. Figure 2 shows a solution of the quartic dispersion equation for TI medium with a tilted angle of 30 degrees, and $\varepsilon = 0.24$ an $\delta = 0.1$. The analytical solutions are also shown in this figure with cyan color. The numerical solutions exactly match them. As in the isotropic PSPI algorithm, several sets of reference parameters must be used for the migration. Ideally, reference wavefields would be generated for each set of reference parameters. Han (2000) put forward the assumption that the anisotropy parameters are tied to reference values of the P-wave velocity. To make computation affordable, it is assumed that parameters v_{p0}, ε and δ have a related lateral variation. Since the tilt angle ϕ has a large effect on the wavefront dip direction, we take full account of the tilted angle.

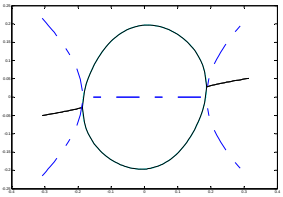

Figure 2. Dispersion relationship of P-wave for a TI medium with 30^0 dipping angle The black solid lines denote the real part of *kz*, the blue dashed lines the are imaginary part of *kz* and the cyan solid lines represent the analytical solutions for the real part of *kz*.

Anisotropic Reverse-time depth migration

It is easy to implement the isotropic reverse-time migration with the acoustic equation. However, for anisotropic reverse-time migration, we should get appropriate P-wave equation first for dipping TI media. Du et al., (2005a) discussed the individual P- and SV-wave equation for dipping TI media. From Equation (1), with the Thomsen approximation and the symmetry axis rotated, the phase velocity of P-waves in dipping TI media is

$$\frac{v_p^2}{v_{p0}^2} = 1 + 2\delta \sin^2(\theta-\phi)\cos^2(\theta-\phi) + 2\varepsilon \sin^4(\theta-\phi) \,. \quad (11)$$

Substituting Equation (10) into Equation (11) and then multiplying it with the wavefields in the wavenumber domain, we can obtain the P-wave equation for tilted TI media:

$$\begin{aligned}\frac{\partial^2 U_p(k_x,k_z,t)}{\partial t^2} = -V_{p0}^2[&k_x^2+k_z^2+(2\delta\sin^2\phi\cos^2\phi+2\varepsilon\cos^4\phi)\frac{k_x^4}{k_x^2+k_z^2}\\ &+(2\delta\sin^2\phi\cos^2\phi+2\varepsilon\sin^4\phi)\frac{k_z^4}{k_x^2+k_z^2}\\ &+(-\delta\sin^2 2\phi+3\varepsilon\sin^2 2\phi+2\delta\cos^2\phi)\frac{k_x^2k_z^2}{k_x^2+k_z^2}\\ &+(\delta\sin 4\phi-4\varepsilon\sin 2\phi\cos^2\phi)\frac{k_x^3k_z}{k_x^2+k_z^2}\\ &+(-\delta\sin 4\phi-4\varepsilon\sin 2\phi\sin^2\phi)\frac{k_z^3k_x}{k_x^2+k_z^2})]U_p(k_x,k_z,t)\end{aligned} \quad . (12)$$

The implementation of prestack anisotropic reverse-time migration is same as that isotropic case. The procedure includes four parts: (1) determine the excitation-time imaging condition by anisotropic ray tracing to obtain traveltime from source position (as for anisotropic Kirchhoff migration), and (2) extrapolate the receiver wavefields, backward in time using the P-wave equation in anisotropic media as shown in Figure 3, and (3) apply the cross-correlated imaging condition.

Performance evaluations

Anisotropic Kirchhoff depth migration differs only in the adjustment of the traveltime calculation as compared with the isotropic case, and the computation of traveltime tables is not related to the depth migration algorithm, so the increase in the computation expense is very small in the whole imaging process. Based on ray theory, it doesn't possess the high accuracy of wave equation migration methods. As for anisotropic PSPI algorithm, from the point of view of wavenumber calculation, there is no obvious improvement in the computer run-time if we obtain the vertical wavenumber before the wavefield extrapolation calculation and make the assumption of anisotropy parameters being related to the lateral velocity. However if it encounters a complicated geometry model with strong variable anisotropy parameters and dipping angles, the method will fail. Although anisotropic reverse-time migration can be well adapted to an arbitrary variable velocity and anisotropy parameters in dipping TI media, it faces a big challenge in computation time. Compared with isotropic algorithm, it almost takes five times a long to run (from the understanding of Equation (12)).

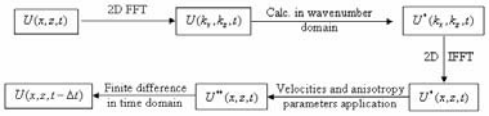

Figure 3. The computation flow for implementing post-stack anisotropic reverse-time migration

Example

To evaluate the three anisotropic migration algorithms, the data is sampled from a model of a TTI thrust sheet in an isotropic background. Dipping structures illustrate the accuracy of steep angle imaging among the accuracy of the three anisotropic depth migration methods. The physical model (Figure 4) is that of a flat reflector overlain by a TI thrust sheet embedded in an isotropic background The thrust sheet is composed of four blocks in the model; each with a unique axis of symmetry. They have parameters of Vp_0 = 2925m/s, $\varepsilon = 0.224$ and $\delta = 0.100$. The isotropic background has a flat basement with Vp_0 = 2740m/s. Isotropic migration results (Du et al., 2005b) produce a partial flat basement, whereas the basement beneath the thrust sheets exhibits substantial pull up and the energy cannot be focused. Migration results from prestack anisotropic Kirchhoff, PSPI and RT migration (Figure 5, Figure 6 and Figure 7) clearly show the flat event and the dipping energy. From the point of view of efficiency, there is only about 5% increase in computer run-time for anisotropic traveltime calculation for the prestack anisotropic Kirchhoff algorithm which is the most efficient migration method. Compared with Kirchhoff and isotropic PSPI methods, prestack anisotropic PSPI has almost more than 50% and 20% additional computation cost. However for anisotropic reverse-time migration, the run-time is increased by almost a factor of 5 compared to the isotropic case. Result is the best image of dipping events in the model (Figure 7), but has the lowest efficiency.

Conclusions

From the above analysis, it is obvious that anisotropy has a large influence on the accuracy of migrated images. Use of a migration algorithm that takes anisotropy into account, with correct velocity information, can substantially improve images when anisotropy is present. In this paper, the prestack anisotropic Kirchhoff, PSPI and reverse-time algorithm theories for TTI media are successfully extended from the isotropic case and introduced here. Prestack anisotropic Kirchhoff depth migration is the most practical method for a certain imaging accuracy. Although prestack anisotropic reverse-time migration shows excellent capability in imaging dipping layers, the calculation time affects its practical implementation. It seems that prestack anisotropic PSPI keeps a good balance between accuracy and efficiency. The assumption about the relationship between the anisotropic parameters and lateral velocities used for the reference wavefield face a challenge in the term of a complex velocity and anisotropic parameters model.

Acknowledgement

Research was funded by the CREWES project and sponsors are thanked for their support. We also would like to give our appreciation to Charles Ursenbach for revising the manuscript.

References

Du, X., Bancroft J. C. and Lines L. R., 2005a, Reverse-time migration for tilted TI media: 75th Mtg. Soc. Expl. Geophys., Expanded Abstracts.

Du, X. Bancroft J. C. and Lines L. R., 2005b, A comparison of anisotropic phase-shift-plus-interpolation and reverse-time depth migration method for tilted TI media, CREWES Report 2005.

Ferguson, R. and Margrave G. F., 1998, Depth migration in TI media by non-stationary phase shift. 68th SEG meeting, New Orleans, U.S.A., Expanded Abstracts, 1831-1834.

Han, B. N., 2000, Two prestack converted-wave migration algorithms for vertical transverse isotropy: 70th Mtg. Soc. Expl. Geophys., Expanded Abstracts.

Isaac, J. H., and Lawton, D. C., 1999, Image mispositioning due to dipping TI media: A physical seismic study: Geophysics, 64, 1230-1238.

Kirtland Grech, M. G., 2002 Depth imagining of fault-fold structures: Ph.D. thesis, University of Calgary

Le Rousseau, J. H., 1991, Phase shift –based migration for transverse isotropy: 61st Mtg. Soc. Expl. Geophys., Expanded Abstracts, 993-996.

Thomsen, L., 1986, Weak elastic anisotropy: Geophysics, 51, 1954–1966.

Tsvankin, I., 1996, P-wave signatures and notation for transversely isotropic media: An overview: Geophysics, 61, 467-483.

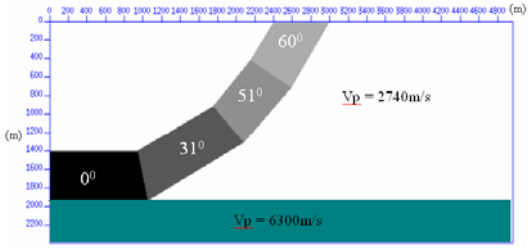

Figure 4: Model of an anisotropic thrust sheet embedded in an isotropic background with same anisotropy parameters and different dipping angles

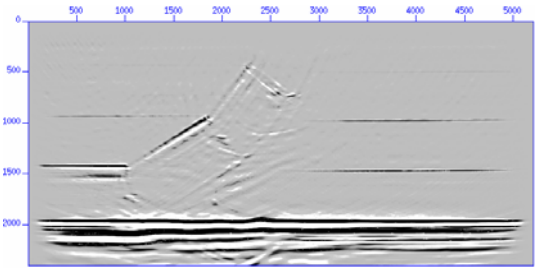

Figure 5: Prestack anisotropic Kirchhoff depth migration result

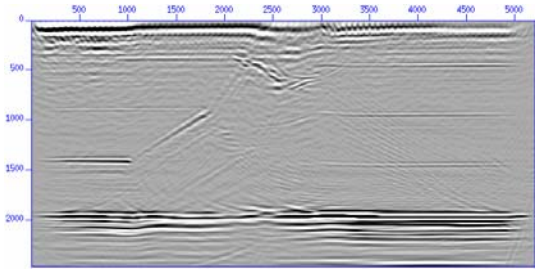

Figure 6: Prestack anisotropic PSPI depth migration result.

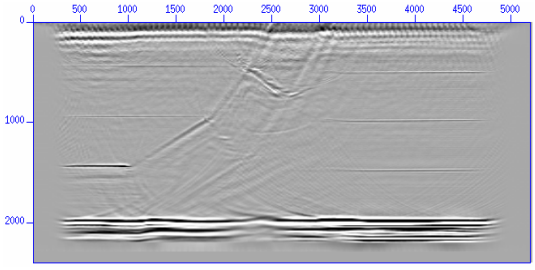

Figure 7: Prestack anisotropic reverse-time depth migration result